applied biosciences

MDPI

Communication

Expedient Access to Type II Kinase Inhibitor Chemotypes by Microwave-Assisted Suzuki Coupling

Lorenza Destro, Ross Van Melsen, Alex Gobbi, Andrea Terzi, Matteo Genitoni and Alfonso Zambon *

Department of Chemical and Geological Sciences, University of Modena and Reggio Emilia, Via G. Campi 103, 41125 Modena, Italy; lorenza.destro@unimore.it (L.D.); rvanmels@unimore.it (R.V.M.); 256915@studenti.unimore.it (A.G.); 229348@studenti.unimore.it (A.T.); 227048@studenti.unimore.it (M.G.)
* Correspondence: alfonso.zambon@unimore.it

Abstract: Functionalized pyrazole-urea scaffolds are a common type II chemotype for the inhibition of protein kinases (PKs), binding simultaneously into the ATP-binding pocket with an ATP bioisostere and into a vicinal allosteric pocket with a pyrazole group. Standard approaches to the scaffold require multi-step synthesis of the ATP bioisostere followed by phosgene or triphosgene-mediated coupling with the substituted pyrazole group. Here we report an expedient approach to the chemotype, characterized by an optimized MW-assisted Suzuki coupling on easily accessed bromo-phenyl pyrazole ureas. The new protocol allowed quick access a large library of target analogues covering a broad chemical space of putative protein kinases inhibitors (PKIs).

Keywords: protein kinase inhibitors; pyrazole-ureas; microwave synthesis

Citation: Destro, L.; Van Melsen, R.; Gobbi, A.; Terzi, A.; Genitoni, M.; Zambon, A. Expedient Access to Type II Kinase Inhibitor Chemotypes by Microwave-Assisted Suzuki Coupling. *Appl. Biosci.* **2022**, *1*, 64–72. https://doi.org/10.3390/applbiosci1010004

Academic Editor: Robert Henry

Received: 29 April 2022
Accepted: 28 May 2022
Published: 31 May 2022

1. Introduction

Protein phosphorylation in eukaryotes plays a key role in cell signaling, gene expression, and differentiation. Protein phosphorylation is also involved in the global control of DNA replication during the cell cycle, as well as in the mechanisms that cope with stress-induced replication blocks [1]. The role of kinases is to phosphorylate serine, threonine, or tyrosine residues of specific protein substrates via the transfer of the γ-phosphate group of adenosine triphosphate (ATP) or, in specific cases, GTP [2]. Protein kinases are, therefore, key enzymes in the function of cellular signaling pathways and are crucial in the regulation of key functions such as cell proliferation, differentiation, and apoptosis [3].

Aberration of PK-mediated cellular pathways is a most common factor in the onset and progression of cancer [4,5], and starting from the early 2000s PKs have emerged as prominent targets for the development of cancer therapies, with 43 protein kinase inhibitors (PKI) approved by FDA for the treatment of solid and liquid tumors [6]. To date, an estimated 20–33% of the global drug discovery efforts are directed at the development of protein kinase inhibitors [7–11]. Depending on their binding mode within the ATP binding site and in proximal or distal allosteric pockets, PKIs are classified as Type I, Type I 1/2, and Type II-VI, with Type I and Type II being first binding modes identified and the most common ones [12]. Type II inhibitors, in particular, bind simultaneously to the ATP-binding pocket and to an adjacent allosteric pocket when the kinase in an inactive, DFG-out conformation, in contrast with Type I inhibitors that bind to the active, DFG-in conformation of the kinase and only into the ATP-binding pocket. Of the 27 co-crystal structures of FDA-approved PKIs available in 2019, eight were Type II [6]. As inactive protein kinase conformations exhibit greater structural variation than the conserved active conformation to which Type I PKIs bind, Type II PKIs are considered potentially more selective than Type I ones [13,14]. Most Type II PKIs share a common chemotype enticing a hydrophobic element that forms Van der Waals interactions with the allosteric pocket and a bridge system (e.g., an amine or a urea) able to form hydrogen bonds with the conserved

salt bridge adjacent to the PK active site and an ATP bioisostere that occupies the ATP binding pocket [15–18].

The introduction of a pyrazole-urea moiety as an allosteric binder in Type II PKIs has been shown to confer activity against a range of protein targets and to improve the pharmacokinetic properties of the scaffold, allowing for the progression to the clinic of several compounds of this type. The general structure of pyrazole-urea PKIs entices a central pyrazole-phenyl urea core substituted on the pyrazole by aliphatic (X) and aromatic and aliphatic (Y) groups and bearing on the phenyl ring a range of substituents usually comprising a variously substituted aromatic group (Z), as depicted in Figure 1 [19–21].

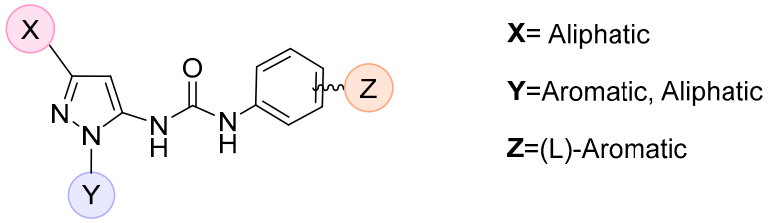

Figure 1. General structure of Type II pyrazole-urea PKI.

In general, access to this chemotype requires the multi-step synthesis of the aniline ATP isostere followed by phosgene or triphosgene-mediated coupling to urea with the pyrazole group. This approach requires lengthy synthetic and purification procedures, the optimization of reaction conditions for each analogue, and the use of hazardous reagents for the coupling step, which often occurs with sub-optimal yields [22–27]. We posit that direct reaction of the pyrazole group with commercial Bromophenyl Isocyanates followed by a Suzuki coupling (Scheme 1) would provide an expedient access to this chemotype. Diversity points can be easily introduced at each step, allowing for the rapid synthesis of a library of analogues [28,29].

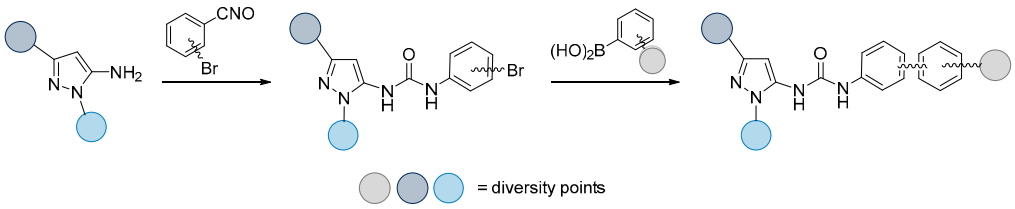

Scheme 1. Proposed route to pyrazole-ureas analogues.

Suzuki-Miyaura coupling allows the formation of new C-C bonds between an aryl halide and an aryl boron species and is particularly suitable for our purpose due to its robustness and tolerance of functional groups. Although this reaction has already been extensively investigated, reactions on substrates containing an aromatic urea group are scantly reported, and no examples in which one of the two aromatic rings is a pyrazole are reported in the literature [30,31] The affinity of palladium for the urea group suggests a possible coordination of the catalyst by our substrate, and thus possible deactivation of the former. Here we report the optimization of the problematic Suzuki-Muyara reaction on pyrazole ureas, and the consequent synthesis of a library of analogues easily accessed by the variation of substituents on the pyrazole and phenylboronic reagents.

2. Materials and Methods

General Methods: Commercial building blocks, reagents, and solvents for reactions were reagent grade and used as purchased or purified according to methods in the literature. Reactions were monitored by Pre-coated TLC sheets ALUGRAM® Sil G/UV$_{254}$ (0.20 mm thickness). Dry solvents were prepared by overnight standing on freshly activated 4 Å molecular sieves under argon atmosphere or purchased. Flash chromatography was

conducted using a Merk 60, 230–400 mesh silica gel. ^{1}H- and ^{13}C-NMR spectra were recorded at 298K on Bruker FT-NMR Advance 400 (400.13 MHz) e Bruker FT-NMR Advance III HD 600 (600.13 MHz). Chemical shift values are given in ppm relative to TMS and were determined by taking as reference the isotopic impurity signals of $CDCl_3$ (7.26 ppm for ^{1}H and 77.16 for ^{13}C) and DMSO-d_6 (2.50 ppm for ^{1}H and 39.52 ppm for ^{13}C). Data are presented as follows: chemical shift (δ) in ppm, multiplicity, coupling constants (J) given in hertz. LCMS data were acquired using a 6130A quadrupole ion trap analyzer Ion Trap LC-MS(n) by Agilent Technologies. Docking analysis was carried out using the Glide Docking Module of Maestro (Schroedinger) in the standard precision (SP) mode.

Detailed synthetic procedures and full characterization of all the synthesized compounds are reported in Supplementary Information.

3. Results

As discussed above, Suzuki coupling on aromatic ureas is rarely reported, and to our knowledge never on a substituted pyrazole scaffold [30,31]. We thus set out to optimize the coupling step using as model reaction the coupling of easily obtained 1-(4-bromophenyl)-3-(3-(tert-butyl)-1-phenyl-1H-pyrazol-5-yl)urea **1a** with boronic 3,4-dimethoxyphenylboronic acid **2a** as coupling partner to 1-(3-(tert-butyl)-1-phenyl-1H-pyrazol-5-yl)-3-(3′,4′-dimethoxy-[1,1′-biphenyl]-4-yl)urea **3a** (Table 1). We first tried the protocol reported by Al-Masoudi et al. [30] for structurally close bis-phenyl ureas, carrying out the reaction under reflux with readily available reagents (Entry 1) but did not observe any product formation after 18h. We then tried varying base, catalyst, and solvent system replacing K_2CO_3 with Na_2CO_3 (Entry 2), $Pd(PPh_3)_4$ with $Pd(dppf)Cl_2$ (Entry 3) and finally the solvent with a 1:1=H_2O:DMF mixture (Entry 4). Again, under all the conditions explored we did not observe any conversion to product, suggesting a considerable deactivation of the substrate towards Suzuki coupling under thermal conditions.

We then set out to explore a range of conditions starting from those reported by Brunner et al. [31] in which coupling of phenyl bromo ureas is carried out under microwave (MW) irradiation. The use of MW is known to improve the reaction rates and thus could overcome the deactivation of the system observed under thermal conditions [32]. As the starting conditions, we used MeCN as solvent, $Pd(PPh_3)_4$ as catalyst, Na_2CO_3 as base and run the reaction for 1 h at 100 °C under microwave condition as reported (Entry 5) [32]. Unfortunately, this reaction did not lead to the desired results, most likely due to the poor solubility of urea **1a** in the solvent medium. We then changed the solvent system by replacing the MeCN with a mixture of a 2M aqueous solution of K_2CO_3 and 1,4-dioxane in a ratio of 1:2, in which our urea proved more soluble (Entry 6). Encouragingly, we observed the formation of some product in the reaction mixture, albeit with incomplete conversion and 30% isolated yield. After several attempts, we were then able to further optimize the reaction conditions by changing both the base by switching K_2CO_3 with Na_2CO_3, a slightly stronger base, and the catalyst by replacing $Pd(PPh_3)_4$ with $Pd(dppf)Cl_2$ (Entry 7–8), a catalyst that was proven stable and effective under microwave conditions [33]. We finally identified the best conditions with the use of $Pd(dppf)Cl_2$ as catalyst and Na_2CO_3 as base with complete spectroscopic conversion and 50% yield after chromatography (Entry 9). After identifying the optimal solvent, base, and catalyst, we decided to investigate if the reaction could be performed at lower temperatures (70 °C instead of 100 °C, Entry 10) and with shorter reaction times (45 min instead of 1.25 h, Entry 11). Lowering the temperature significantly affected the conversion, with only 15% of urea **1a** converted to **3a**, but we found that reaction times could be shortened to 30 min (Entry 11), with ~99% conversion of urea **1a** to **3a,** in line with that observed for Entry 9.

Table 1. Optimization of the reaction conditions for the Suzuki coupling of **1a** and **2a**.

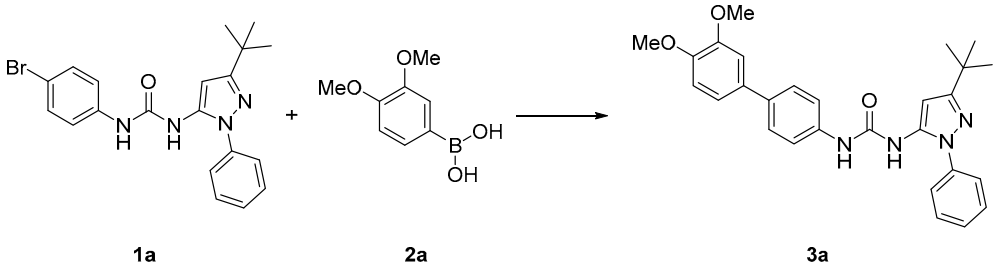

1a **2a** **3a**

Entry	Conditions	Time (h)	T (°C)	Solvent	Catalyst	Base	Yield
1	T_1	18	101	1,4-dioxane	$Pd(PPh_3)_4$	K_2CO_3	N.R.
2	T_2	18	101	1,4-dioxane	$Pd(PPh_3)_4$	Na_2CO_3	N.R.
3	T_3	18	101	1,4-dioxane	$Pd(dppf)Cl_2$	K_2CO_3	N.R.
4	T_4	18	100	1:1 DMF/H_2O	$Pd(PPh_3)_4$	K_2CO_3	N.R.
5	MW	1	100	MeCN	$Pd(PPh_3)_4$	Na_2CO_3	N.R.
6	MW	1.25	100	1:2 H_2O/1,4-dioxane	$Pd(PPh_3)_4$	Na_2CO_3	30% [a]
7	MW	1.25	100	1:2 H_2O/1,4-dioxane	$Pd(PPh_3)_4$	K_2CO_3	N.R.
8	MW	1.25	100	1:2 H_2O/1,4-dioxane	$Pd(dppf)Cl_2$	K_2CO_3	N.R.
9	MW_5	1.25	100	1:2 H_2O/1,4-dioxane	$Pd(dppf)Cl_2$	Na_2CO_3	50% [a]
10	MW_6	1.25	70	1:2 H_2O/1,4-dioxane	$Pd(dppf)Cl_2$	Na_2CO_3	15% [b]
11	MW_7	0.5	100	1:2 H_2O/1,4-dioxane	$Pd(dppf)Cl_2$	Na_2CO_3	~99% [b]

[a] Isolated yield (column purification) [b] spectroscopic yield (^{1}H-NMR) N.R. = Not reacted; only Starting materials recovered.

We then set out to perform the synthesis of a small library of analogues of **1a** taking advantage of the newly optimized Suzuki procedure. Although reaction time could be lowered at 30 min, we deemed it preferable to keep it at 1.25 h to account for the potential lower reactivity of the alternative boronic agents.

The overall synthetic route to this library of compounds is depicted in Scheme 2 and involves the condensation of an oxo nitrile **4a-b** with a hydrazine **5a-c** to give pyrazole **6a-f**, followed by the formation of Br-substituted ureas **1a-h** by reaction with isocyanates **7a-b**. These steps are already well reported in the scientific literature and gave high yields for all the substrates explored [34].

Ureas **1a-l** were finally reacted following the optimized Suzuki protocol with selected boronic acids **2a-e** to afford para-substituted (**3a-f**) and meta-substituted (**3g-l**) final compounds in good 35–60% yields as reported in Table 2 (para-substituted compounds) and Table 3 (meta-substituted compounds).

For a preliminary evaluation of the potential of our compounds as PKIs, we carried out docking of **3a-l** in the co-crystal structure (pdb code 1KV2) of p38, a validated target for autoimmune diseases, with pyrazole-urea BIRB-796 [21]. All compounds faithfully mirrored the binding mode of BIRB-796 and registered high docking scores, suggesting a high affinity of the library for p38 (Figure 2). The best affinities were calculated for compounds **3g**, **3h**, **3l** and **3a**, with docking scores ranging from −11.7 and −8.9 kcal/mol.

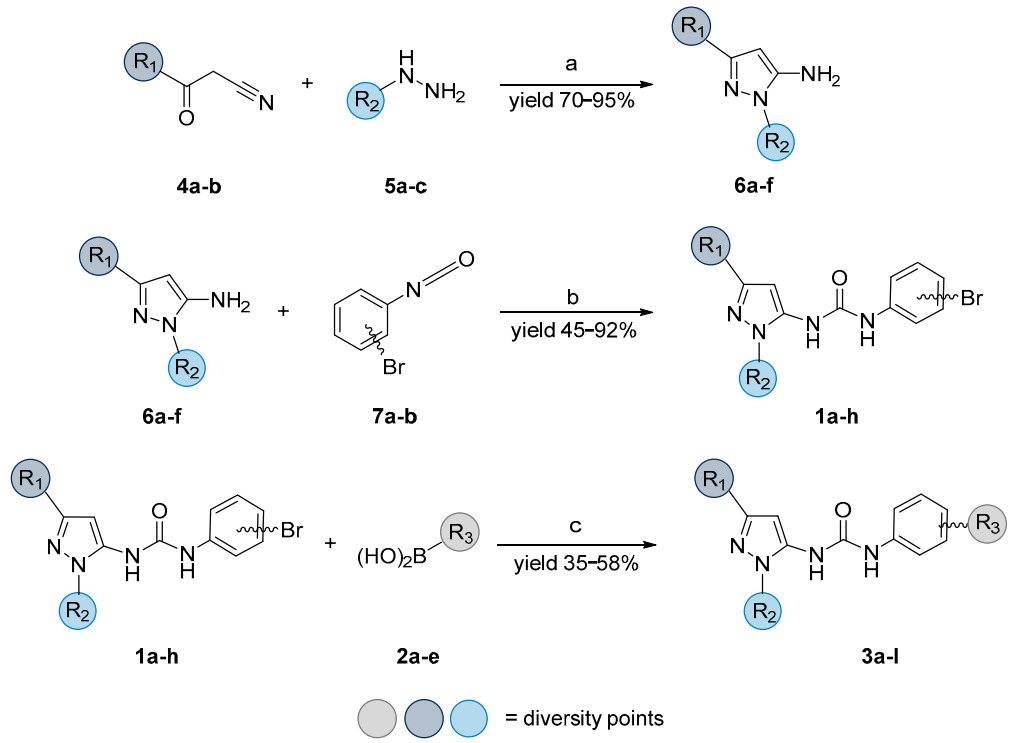

Scheme 2. General synthetic route to pyrazole urea **3a-l**. Reagents and conditions: (**a**) Toluene, 116 °C, 72 h; (**b**) anhydrous DCM, room temperature, 24 h; (**c**) 1:2 H_2O/1,4-dioxane, 100 °C, 1.25 h.

Table 2. Structures and yields of the final step of compounds **3a-f**.

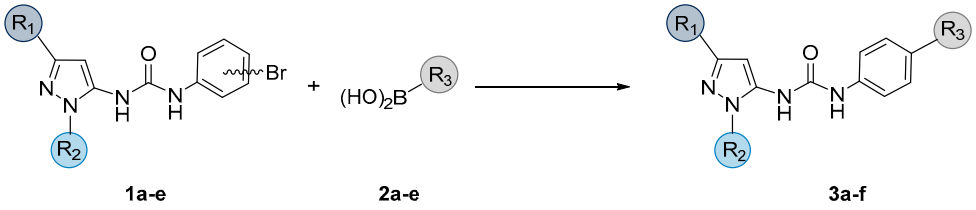

Compound	R_1	R_2	R_3	Yield
3a		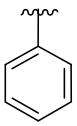	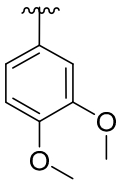	35%
3b		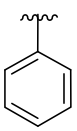	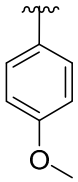	43%
3c		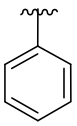	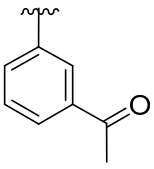	36%

Table 2. *Cont.*

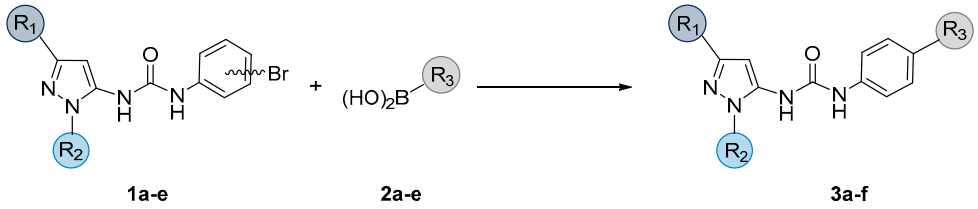

1a-e **2a-e** **3a-f**

Compound	R_1	R_2	R_3	Yield
3d			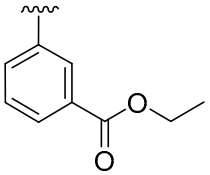	52%
3e		-Me	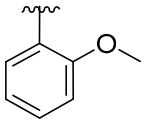	48%
3f		-Me	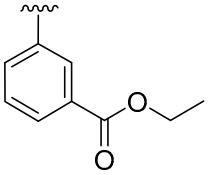	58%

Table 3. Structures and yields of the final step of compounds **3g-l**.

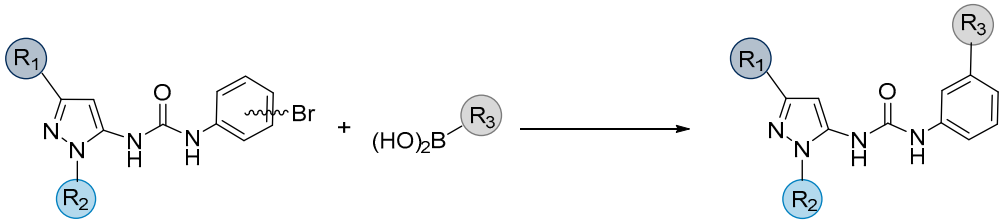

1f-h **2a-c** **3g-l**

Compound	R_1	R_2	R_3	Yield
3g		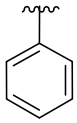	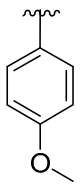	36%
3h		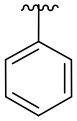	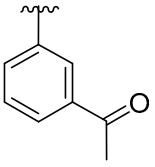	48%

Table 3. *Cont.*

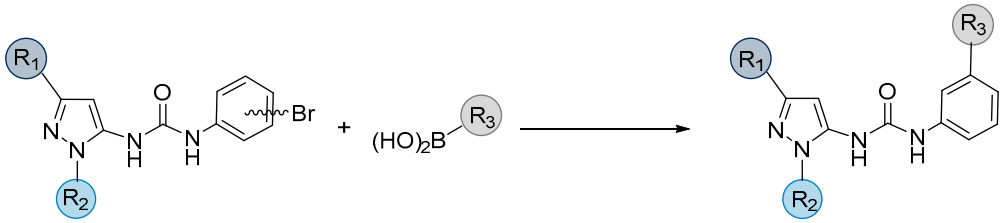

1f-h **2a-c** **3g-l**

Compound	R_1	R_2	R_3	Yield
3i			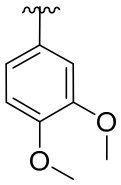	36%
3l		-Me	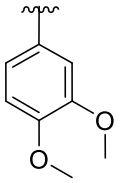	41%

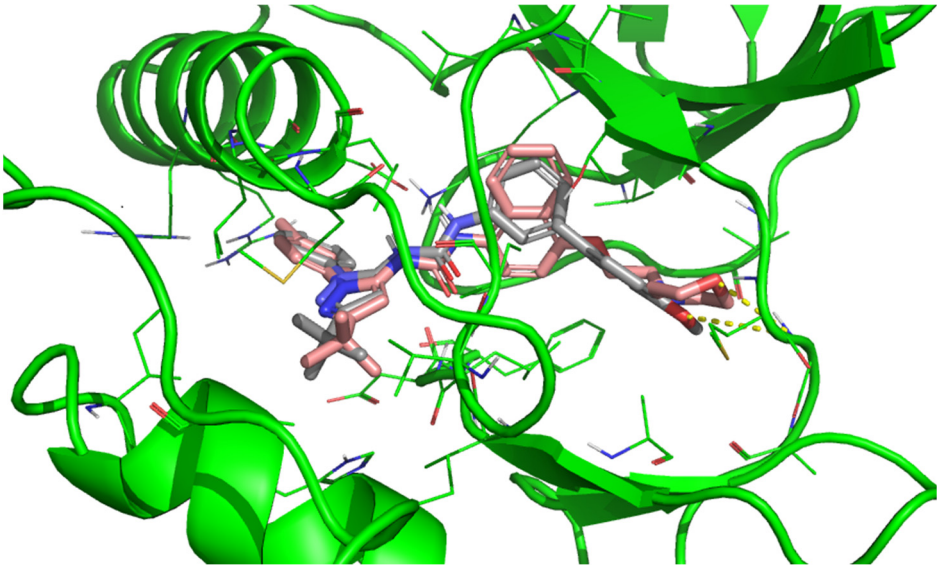

Figure 2. Docking pose of compound 3g (gray) into the binding pocket of p38 (pdb code 1KV2) superposed to BIRB-796 (pink).

4. Conclusions

In conclusion, we report a novel, efficient synthetic route to a privileged scaffold for protein kinase inhibitors based on a novel, robust microwave-assisted protocol for the Suzuki reaction of pyrazole ureas, which allowed quick to access a structurally varied library of putative kinase inhibitors. Although this route is limited to the synthesis of biphenyl pyrazole ureas, it compares favorably with previous literature in terms of yields and overall ease of synthesis.

Supplementary Materials: The following supporting information can be downloaded at: https://www.mdpi.com/article/10.3390/applbiosci1010004/s1.

Author Contributions: Conceptualization, L.D. and A.Z.; methodology, L.D., A.Z. and R.V.M.; validation, L.D. and A.Z.; investigation, L.D., R.V.M., M.G., A.T., A.G. and A.Z.; resources, L.D. and A.Z.; data curation, L.D. and A.Z.; writing—original draft, L.D. and A.Z.; writing—review & editing Preparation, L.D., R.V.M., M.G., A.T. and A.Z.; supervision, A.Z. All authors have read and agreed to the published version of the manuscript.

Funding: This research received no external funding.

Institutional Review Board Statement: Not applicable.

Informed Consent Statement: Not applicable.

Conflicts of Interest: The authors declare no conflict of interest.

References

1. Garcia, T.G.; Poncet, S.; Derouiche, A.; Shi, L.; Mijakovic, I.; Noirot-Gros, M.-F. Role of Protein Phosphorylation in the Regulation of Cell Cycle and DNA-Related Processes in Bacteria. *Front. Microbiol.* **2016**, *7*, 184. [CrossRef]
2. Niefind, K.; Pütter, M.; Guerra, B.; Issinger, O.G.; Schomburg, D. GTP plus water mimic ATP in the active site of protein kinase CK2. *Nat. Genet.* **1999**, *6*, 1100–1103. [CrossRef]
3. Huse, M.; Kuriyan, J. The Conformational Plasticity of Protein Kinases. *Cell* **2002**, *109*, 275–282. [CrossRef]
4. Hanahan, D.; Weinberg, R.A. The Hallmarks of Cancer. *Cell* **2000**, *100*, 57–70. [CrossRef]
5. Hanahan, D.; Weinberg, R.A. Hallmarks of cancer: The next generation. *Cell* **2011**, *144*, 646–674. [CrossRef]
6. Roskoski, R. Properties of FDA-approved small molecule protein kinase inhibitors. *Pharmacol. Res.* **2019**, *144*, 19–50. [CrossRef]
7. Ferguson, F.M.; Gray, N.S. Kinase inhibitors: The road ahead. *Nat. Rev. Drug Discov.* **2018**, *17*, 353–377. [CrossRef]
8. Wu, P.; Nielsen, T.E.; Clausen, M.H. Small-molecule kinase inhibitors: An analysis of FDA-approved drugs. *Drug Discov. Today* **2016**, *21*, 5–10. [CrossRef]
9. Liao, J.J.-L. Molecular Recognition of Protein Kinase Binding Pockets for Design of Potent and Selective Kinase Inhibitors. *J. Med. Chem.* **2007**, *50*, 409–424. [CrossRef]
10. Attwood, M.M.; Fabbro, D.; Sokolov, A.V.; Knapp, S.; Schiöth, H.B. Trends in kinase drug discovery: Targets, indications and inhibitor design. *Nat. Rev. Drug Discov.* **2021**, *20*, 839–861. [CrossRef]
11. Cohen, P.; Cross, D.; Jänne, P.A. Kinase drug discovery 20 years after imatinib: Progress and future directions. *Nat. Rev. Drug Discov.* **2021**, *20*, 551–569. [CrossRef]
12. Roskoski, R., Jr. Classification of small molecule protein kinase inhibitors based upon the structures of their drug-enzyme complexes. *Pharmacol. Res.* **2016**, *103*, 26–48. [CrossRef]
13. Mol, C.D.; Fabbro, R.; Hosfield, D.J. Structural insights into the conformational selectivity of STI-571 and related kinase inhibitors. *Curr. Opin. Drug Discov. Dev.* **2004**, *7*, 639–648.
14. Vijayan, R.S.K.; He, P.; Modi, V.; Duong-Ly, K.C.; Ma, H.; Peterson, J.R.; Dunbrack, J.R.L.; Levy, R.M. Conformational Analysis of the DFG-Out Kinase Motif and Biochemical Profiling of Structurally Validated Type II Inhibitors. *J. Med. Chem.* **2015**, *58*, 466–479. [CrossRef]
15. Treiber, D.K.; Shah, N.P. Ins and Outs of Kinase DFG Motifs. *Chem. Biol.* **2013**, *20*, 745–746. [CrossRef]
16. Zhao, Z.; Wu, H.; Wang, L.; Liu, Y.; Knapp, S.; Liu, Q.; Gray, N.S. Exploration of type II binding mode: A privileged approach for kinase inhibitor focused drug discovery? *ACS Chem. Biol.* **2014**, *9*, 1230–1241. [CrossRef]
17. Zuccotto, F.; Ardini, E.; Casale, E.; Angiolini, M. Through the "Gatekeeper Door": Exploiting the Active Kinase Conformation. *J. Med. Chem.* **2009**, *53*, 2681–2694. [CrossRef]
18. Chahrour, O.; Cairns, D.; Omran, Z. Small molecule kinase inhibitors as anti-cancer therapeutics. *Mini-Rev. Med. Chem.* **2012**, *12*, 399–411. [CrossRef]
19. Saturno, G.; Lopes, F.; Niculescu-Duvaz, I.; Zambon, A.; Davies, L.; Johnson, L.; Preece, N.; Lee, R.; Viros, A.; Holovanchuk, D.; et al. The paradox-breaking panRAF plus SRC family kinase inhibitor, CCT3833, is effective in mutant KRAS-driven cancers. *Ann. Oncol.* **2021**, *32*, 269–278. [CrossRef]
20. Girotti, M.R.; Lopes, F.; Preece, N.; Niculescu-Duvaz, D.; Zambon, A.; Davies, L.; Whittaker, S.; Saturno, G.; Viros, A.; Pedersen, M.; et al. Paradox-Breaking RAF Inhibitors that Also Target SRC Are Effective in Drug-Resistant BRAF Mutant Melanoma. *Cancer Cell* **2015**, *27*, 85–96. [CrossRef]
21. Pargellis, C.; Tong, L.; Churchill, L.; Cirillo, P.F.; Gilmore, T.; Graham, A.G.; Grob, P.M.; Hickey, E.R.; Moss, N.; Pav, S.; et al. Inhibition of p38 MAP kinase by utilizing a novel allosteric binding site. *Nat. Genet.* **2002**, *9*, 268–272. [CrossRef] [PubMed]
22. Niculescu-Duvaz, D.; Gaulon, C.; Dijkstra, H.P.; Niculescu-Duvaz, I.; Zambon, A.; Ménard, D.; Suijkerbuijk, B.M.J.M.; Nourry, A.; Davies, L.; Manne, H.; et al. Pyridoimidazolones as Novel Potent Inhibitors of v-Raf Murine Sarcoma Viral Oncogene Homologue B1 (BRAF). *J. Med. Chem.* **2009**, *52*, 2255–2264. [CrossRef] [PubMed]

23. Suijkerbuijk, B.M.J.M.; Niculescu-Duvaz, I.; Gaulon, C.; Dijkstra, H.P.; Niculescu-Duvaz, D.; Ménard, D.; Zambon, A.; Nourry, A.; Davies, L.; Manne, H.A.; et al. Development of Novel, Highly Potent Inhibitors of V-RAF Murine Sarcoma Viral Oncogene Homologue B1 (BRAF): Increasing Cellular Potency through Optimization of a Distal Heteroaromatic Group. *J. Med. Chem.* **2010**, *53*, 2741–2756. [CrossRef] [PubMed]
24. Zambon, A.; Ménard, D.; Suijkerbuijk, B.M.J.M.; Niculescu-Duvaz, I.; Whittaker, S.; Niculescu-Duvaz, D.; Nourry, A.; Davies, L.; Manne, H.A.; Lopes, F.; et al. Novel Hinge Binder Improves Activity and Pharmacokinetic Properties of BRAF Inhibitors. *J. Med. Chem.* **2010**, *53*, 5639–5655. [CrossRef]
25. Whittaker, S.; Ménard, D.; Kirk, R.; Ogilvie, L.; Hedley, D.; Zambon, A.; Lopes, F.; Preece, N.; Manne, H.; Rana, S.; et al. A novel, selective, and efficacious nanomolar pyridopyrazinone inhibitor of V600EBRAF. *Cancer Res.* **2010**, *70*, 8036–8044. [CrossRef]
26. Zambon, A.; Niculescu-Duvaz, D.; Niculescu-Duvaz, I.; Marais, R.; Springer, C.J. BRAF as a therapeutic target: A patent review (2006–2012). *Expert Opin. Ther. Pat.* **2013**, *23*, 155–164. [CrossRef]
27. Gennäs, G.B.A.; Mologni, L.; Ahmed, S.; Rajaratnam, M.; Marin, O.; Lindholm, N.; Viltadi, M.; Gambacorti-Passerini, C.; Scapozza, L.; Yli-Kauhaluoma, J. Design, Synthesis, and Biological Activity of Urea Derivatives as Anaplastic Lymphoma Kinase Inhibitors. *ChemMedChem* **2011**, *6*, 1680–1692. [CrossRef]
28. Suzuki, A. Organoborates in new synthetic reactions. *Accounts Chem. Res.* **2002**, *15*, 178–184. [CrossRef]
29. Miyaura, N.; Yanagi, T.; Suzuki, A. The Palladium-Catalyzed Cross-Coupling Reaction of Phenylboronic Acid with Haloarenes in the Presence of Bases. *Synth. Commun.* **2006**, *11*, 513–519. [CrossRef]
30. Al-Masoudi, N.A.; Essa, A.H.; Alwaaly, A.A.; Saeed, B.A.; Langer, P. Synthesis and conformational analysis of new arylated-diphenylurea derivatives related to sorafenib drug via Suzuki-Miyaura cross-coupling reaction. *J. Mol. Struct.* **2017**, *1146*, 522–529. [CrossRef]
31. Brunner, K.; Maric, S.; Reshma, R.S.; Almqvist, H.; Seashore-Ludlow, B.; Gustavsson, A.-L.; Poyraz, O.; Yogeeswari, P.; Lundbäck, T.; Vallin, M.; et al. Inhibitors of the Cysteine Synthase CysM with Antibacterial Potency against Dormant Mycobacterium tuberculosis. *J. Med. Chem.* **2016**, *59*, 6848–6859. [CrossRef] [PubMed]
32. Dudley, G.B.; Richert, R.; Stiegman, A.E. On the existence of and mechanism for microwave-specific reaction rate enhancement. *Chem. Sci.* **2015**, *6*, 2144–2152. [CrossRef] [PubMed]
33. Zhang, W.; Chen, C.H.-T.; Lu, Y.; Nagashima, T. A Highly Efficient Microwave-Assisted Suzuki Coupling Reaction of Aryl Perfluorooctylsulfonates with Boronic Acids. *Org. Lett.* **2004**, *6*, 1473–1476. [CrossRef] [PubMed]
34. Regan, J.; Breitfelder, S.; Cirillo, P.; Gilmore, T.; Graham, A.G.; Hickey, E.; Klaus, B.; Madwed, J.; Moriak, M.; Moss, N.; et al. Pyrazole Urea-Based Inhibitors of p38 MAP Kinase: From Lead Compound to Clinical Candidate. *J. Med. Chem.* **2002**, *45*, 2994–3008. [CrossRef]